

PR/11/76

2001093554  
WILL BE SUBMITTED TO  
JOURNAL OF APPLIED PHYSICS  
523779

## The Single-crystal Elasticity of Yttria ( $Y_2O_3$ ) to High Temperature

James W. Palko and Waltraud M. Kriven

Department of Materials Science and Engineering, University of Illinois, Urbana,  
IL 61801

Stanislav V. Sinogeikin and Jay D. Bass

Department of Geology, University of Illinois, Urbana, IL 61801

Ali Sayir

NASA Glenn Research Center, Cleveland, OH 44135

The single-crystal elastic moduli of yttria have been measured by Brillouin spectroscopy up to 1200 °C. The room temperature values obtained are  $C_{11} = 223.6 \pm 0.6$  GPa,  $C_{44} = 74.6 \pm 0.5$  GPa, and  $C_{12} = 112.4 \pm 1.0$  GPa. The resulting bulk and (Voigt-Reuss-Hill) shear moduli are  $K = 149.5 \pm 1.0$  GPa and  $G_{VRH} = 66.3 \pm 0.8$  GPa, respectively. These agree much more closely with experimental values reported for polycrystalline samples than do previous single-crystal measurements. Linear least squares regressions to the variation of bulk and shear moduli with temperature result in derivatives of  $dK/dT = -17 \pm 2$  MPa/°C and  $dG_{VRH}/dT = -8 \pm 2$  MPa/°C. Elastic anisotropy was found to remain essentially constant over the temperature range studied.

PACS numbers: 62.20.Dc

## I. Introduction

Yttria, or yttrium sesquioxide ( $Y_2O_3$ ), is a refractory material with a cubic crystal structure.<sup>1</sup> Yttria, in the form of dense polycrystalline ceramics, has been considered for use in nuclear applications<sup>2</sup> and has gained interest relatively recently for use in infrared optics.<sup>1,3,4</sup> Due to yttria's optical isotropy (resulting from its cubic structure), it is possible that, in the future, optical components requiring high quality may be made from single crystals. The single-crystal elastic moduli are valuable for designing such optical components. In particular, the temperature derivatives of elastic moduli allow dimensional changes due to heating under physical constraint, as well as acoustic excitation to be determined. The single-crystal elastic moduli are also useful in understanding the fundamental physics of yttria. Single-crystal yttria fibers suitable for such elasticity measurements have recently been produced using a laser-heated, float zone technique.<sup>5</sup>

The elastic properties of pure and doped polycrystalline yttria have been determined by several authors<sup>6-13</sup> including measurements to high temperatures.<sup>1,2,14</sup> In addition, single-crystal measurements have been reported at room temperature.<sup>15,16</sup> There are, however, significant discrepancies between the bulk and shear moduli reported for dense polycrystalline materials and those calculated from the previously reported single-crystal moduli. The purpose of this study was to obtain accurate values of the single crystal elastic moduli of  $Y_2O_3$  both at room and elevated temperatures.

Brillouin scattering offers a convenient means of measuring the complete set of elastic moduli for single crystals, especially at elevated temperatures. It requires no

physical contact with the sample, is capable of measuring along numerous crystallographic directions in a single sample, and requires only small sample volumes. Brillouin scattering arises from the inelastic scattering of photons from acoustic phonons in the sample. The scattered light is shifted in frequency with respect to the incident light by a factor that is proportional to the velocity of the acoustic waves (Eq. 1).<sup>17</sup>

$$V = \left( \frac{\Delta\omega}{\omega} \right) \left( \frac{c}{2n \sin(\theta/2)} \right) \quad (1)$$

Here  $V$  is the velocity of an acoustic wave,  $\Delta\omega$  is the frequency shift of the scattered light,  $\omega$  is the frequency of the incident light,  $c$  is the speed of light,  $n$  is the index of refraction of the sample, and  $\theta$  is the scattering angle. In this study, we employed a special case of symmetric scattering called platelet geometry (Figure 1), which utilizes a sample with flat, parallel faces and equal angles between the face normals and incident/scattered beam directions. The phonon propagation direction  $q$  is in the plane of the sample, and the face normals as well as the incident/scattered light rays all lie within a plane.<sup>18</sup> Figure 1 shows a schematic of symmetric platelet scattering. With symmetric platelet scattering geometry, the scattering angle is easily defined, and no knowledge of the index of the refraction of the sample is necessary. As seen in Figure 1, Snell's law allows the replacement of  $n \sin(\theta/2)$  with  $n_o \sin(\theta_o/2)$  in Eq. 1. This is particularly beneficial for high

temperature studies where the variation of index of refraction with temperature is generally unknown and difficult to measure.

The elastic waves may be treated by a continuum mechanical analysis which relates their velocities along a given crystallographic direction to the adiabatic elastic moduli and density of the material via Christoffel's equation (Eq. 2).<sup>19</sup>

$$\left| C_{ijkl}q_jq_l - \rho V^2 \delta_{ik} \right| = 0 \quad (2)$$

$C_{ijkl}$  is the elasticity tensor for the material,  $\rho$  is the density, and  $\delta_{ik}$  is the Krönecker delta function. Since yttria has cubic symmetry, there are only three independent, nonzero components in its elasticity tensor,  $C_{11}(=C_{22}=C_{33})$ ,  $C_{12}(=C_{13}=C_{23})$ , and  $C_{44}(=C_{55}=C_{66})$  (in Voigt notation).<sup>20</sup>

## II. Experiment

### A. Samples

Samples for this study were taken from single-crystal fibers grown from high purity  $Y_2O_3$  powder by a laser heated float zone (LHFZ) technique.<sup>5,21</sup> This containerless technique uses a scanned  $CO_2$  laser beam (10.6  $\mu m$  wavelength) that is split and focused at the tip of a polycrystalline source rod to produce a melt which is held between the source and product phases by surface tension. Temperature in the molten

region was stabilized using infrared pyrometry, but absolute temperature was not determined because the emissivity of molten yttria is not known.

For preparation of the source rod, high purity (99.999% pure) polycrystalline yttria powder (Alpha Aesar) was used. Since the LHFZ technique is essentially a zone refining process, the final purity of the yttria crystal is likely even higher. This powder was blended with 5 weight % binder (Methocel 20-231, The Dow Chemical Company, Midland, MI 48674) and glycerin was used as a plasticizer in a water based slurry. The slurry was then degassed overnight with a moderate vacuum ( $\sim 70 \times 10^3$  Pa) to achieve a high viscosity paste. This paste was extruded with a custom-made mini-extruder, i.e. a modified hypodermic syringe. The plastic syringe wall was replaced within high wear regions to avoid contamination. At least two extrusions were made to minimize porosity in the paste. The extruded source rod was normally 250  $\mu\text{m}$  in diameter and extruded lengths were 15 to 20 cm long. The rods were furnace dried in air at 200  $^\circ\text{C}$  for approximately 1 hour and placed in the LHFZ apparatus without any presintering.

At steady state, the source to fiber diameter ratio is inversely proportional to the square root of the feed rod to pull rod velocity ratio. The fibers used for the Brillouin work had nearly circular cross sections with average diameters slightly less than 500  $\mu\text{m}$ . For fibers grown in this study, the molten zone height was kept constant at approximately one and half times the fiber diameter, and fibers were grown in air.

Octahedral cleavage was apparent in fragments broken from the fibers and showed that the fiber axis coincided closely with the  $\langle 111 \rangle$  crystal direction. The material was clear except for occasional inclusions that appear to be bubbles. The

samples were optically isotropic when examined under cross polarized light. An X-ray analysis was performed on a large fiber sample by four circle diffractometry, in order to verify the single-crystal nature and cubic symmetry of the samples. Precise values of the lattice parameter at all temperatures were calculated from the regression equation of Taylor (Eq. 3),<sup>22</sup>

$$a(T) = (1.06016 \text{ nm}) (1 + 6.76 \times 10^{-6} T + 1.22 \times 10^{-9} T^2) \quad (3)$$

where  $a(T)$  is the cell edge parameter at a temperature  $T$  (in °C). A value of 1.0603 nm (corresponding to 22°C) yielding a theoretical density of 5.033 g/cm<sup>3</sup> (which matches that reported by Tropf and Harris<sup>1</sup>) was used for all room temperature calculations.

Velocity measurements were performed on a single sample. It was ground into a flat plate with a thickness of ~150 μm.<sup>23</sup> Due to breakage during sample preparation, the usable area of the sample faces was around 250 μm x 250 μm. The ground faces corresponded closely to the {100} crystallographic plane. Orientation was accomplished by optical goniometry from cleavage planes, and measurements subsequent to grinding showed the face to be within ~2° of the {100} face.

## B. Brillouin Scattering

Illumination of the sample was provided by the 514.5 nm line of an Ar<sup>+</sup> laser at a power of 200 mW or less for the ambient temperature measurements. For high temperature runs, a laser power of up to 400 mW was used to maximize the Brillouin

signal since sample heating was not a particular concern. Higher power was necessary for high temperature experiments because of the furnace windows which reduce the intensities of both the incident and scattered beams by partial reflection and introduction of astigmatism into the focusing and collecting optical paths. Scattered light was collected through a slot with an angular acceptance of approximately  $5.5^\circ$  in the scattering plane to lessen broadening of Brillouin peaks. The scattered light was analyzed by a 6-pass, tandem, Fabry-Perot interferometer. The spectrometer has been described in detail elsewhere.<sup>24,25</sup>

Room temperature measurements were performed with a  $90^\circ$  scattering angle. An Eulerian cradle was used to rotate the sample around its face normal to access different phonon directions. The high temperature results of this study were obtained using a compact furnace mounted on the Eulerian cradle, allowing multiple phonon directions to be collected without remounting the sample. The construction and operation of this furnace is described elsewhere.<sup>26</sup> An  $80^\circ$  scattering angle was used for the high temperature work. Velocities calculated from the measured Brillouin shifts were used in a linearized inversion algorithm<sup>27</sup> to solve for the elastic moduli.

### III. Results and Discussion

Velocities measured at room temperature, in the plane  $\sim(001)$  (outside the furnace), have a close correspondence to fits from the calculated elastic constants (solid curves Figure 2). This figure gives a sense of the anisotropy in yttria. Longitudinal velocities vary by  $\sim 4\%$  in this plane, while shear velocities vary by  $\sim 15\%$ .

The adiabatic elastic constants obtained are given in Table I along with those reported by Aleksandrov et al. (also measured using Brillouin spectroscopy)<sup>15,16</sup> Errors in Table I include contributions due to residuals of the velocity fits as well as uncertainty in sample orientation.<sup>23</sup> There are substantial differences between Aleksandrov's values and those obtained here ( $C_{11}$  +1.5%,  $C_{44}$  -8%,  $C_{12}$  +20%). Table II lists the bulk modulus,  $K$ , and shear modulus,  $G$ , calculated from the room temperature constants using the Voigt, Reuss, and Voigt-Reuss-Hill averaging schemes (denoted by subscripts V, R, and VRH respectively) for both this study and for Aleksandrov et al. For comparison, values of  $K$  and  $G$  (adiabatic) reported previously by several authors for polycrystalline yttria are included in Table II. The values reported by Manning<sup>8</sup> are a Spriggs extrapolation to zero porosity from samples with porosity ranging from 4-22 %, whereas those of Yeheskel<sup>13</sup> and Tropsch<sup>1</sup> are uncorrected, and correspond to samples of greater than 99% theoretical density. This fact may account for the differences in bulk modulus.

The values of Aleksandrov et al.<sup>15,16</sup> for  $K$  and  $G_{VRH}$  are 11% higher and 14% lower, respectively, than those reported here. Clearly, the current measurements agree much more closely with polycrystalline measurements than those of Aleksandrov et al. No details of the quality or properties of the sample are reported in the previous single crystal study,<sup>15</sup> but these aspects may partially account for some of the discrepancies. Another possible explanation is a misorientation of the sample used in the previous study. The differences decrease in the order:  $|\Delta C_{12}/C_{12}| > |\Delta C_{44}/C_{44}| > |\Delta C_{11}/C_{11}|$ . Ingel and Lewis derived a similar relation of relative magnitudes of deviation for misorientation in  $Y_2O_3$  stabilized  $ZrO_2$  along certain directions.<sup>28</sup> Aleksandrov et al. calculated moduli

based on the longitudinal and shear (degenerate) velocities along [100] for which the reported values are  $6.75 \pm 0.02$  km/s and  $3.71 \pm 0.03$  km/s, respectively, as well as both shear velocities along  $[0.5 \ 0.5 \ 1/\sqrt{2}]$  which are reported as  $3.43 \pm 0.02$  km/s and  $3.69 \pm 0.01$  km/s.<sup>15</sup> Similar velocities result from Eq. 2 using the elastic moduli determined in this study, if a rotation of  $\sim 13^\circ$  around [010] is applied to the coordinates of Aleksandrov et al. (i.e. [100] becomes [0.9744 0 0.2250], and  $[0.5 \ 0.5 \ 1/\sqrt{2}]$  becomes [0.3281 0.5 0.8015].) The resulting longitudinal and shear velocities along [0.9744 0 0.2250] are 6.726 km/s and 3.745 km/s. (The other shear mode with a velocity of 3.849 km/s is polarized along [010]. Since the incident and scattered beams were directed along [110] and [-110] (in the original coordinate system),<sup>15</sup> this wave is polarized in the scattering plane and would have zero scattered intensity.<sup>29</sup>) The shear velocities along [0.3281 0.5 0.8015] are 3.710 km/s and 3.454 km/s. Aleksandrov et al. report the accuracy of face orientation as 3 to 5°,<sup>15</sup> but this degree of misorientation cannot account for the differences with the current study.

The variation of the single-crystal elastic moduli with temperature is consistent with a linear trend as shown by Figure 3. Table III lists values for the adiabatic constants determined at elevated temperatures. Errors given again include contributions from residuals in the fit as well as uncertainty in sample orientation.<sup>23</sup> Higher order polynomial fits to these results are not warranted, given the uncertainties in the data. The temperature derivatives of the elastic moduli from the linear fits are listed in Table IV along with those for the bulk modulus and Voigt-Reuss-Hill shear modulus. Errors in the temperature derivatives are based on the 95% confidence intervals for the slope of the

linear fit. An error of  $\pm 5\%$  is given in temperature itself based on uncertainty in the gain of the amplifier used in measuring temperature. This may contribute to an absolute error in slope, but the internal temperature precision is much better ( $< 3\%$ ).<sup>23</sup> Furthermore, the uncertainty in slope is dominated by errors in velocity, not in temperature.

Figures 4 and 5 show the temperature dependence of bulk and shear (Voigt-Reuss-Hill) moduli respectively. Also shown are values measured by Dickson and Anderson using a resonance technique (resulting in adiabatic moduli) on a  $0.91 \text{ Y}_2\text{O}_3 \cdot 0.09 \text{ ThO}_2$  polycrystalline sample.<sup>14</sup> There is a slight offset in bulk modulus, but the rate of softening with temperature is similar for both materials. Linear fits to the data of Dickson and Anderson<sup>14</sup> yield slopes of  $-15.3 \text{ MPa/}^\circ\text{C}$  and  $-8.5 \text{ MPa/}^\circ\text{C}$  for bulk and shear modulus respectively. The offset in bulk modulus may be due to composition, but no estimate of possible errors is given by Dickson and Anderson<sup>14</sup> so the differences may be insignificant.

Figure 6 shows the Young's modulus for yttria calculated from Eq. 4,

$$E = \frac{9KG_{\text{VRH}}}{3K + G_{\text{VRH}}} \quad (4)$$

along with the data of Price and Hubbert,<sup>30</sup> Dickson and Anderson,<sup>14</sup> a linear fit to the data of Marlowe and Wilder up to  $1000^\circ\text{C}$ ,<sup>2</sup> and a fit suggested by Tropf and Harris<sup>1</sup> (based on data from Price and Hubbert<sup>30</sup>). The fit to the data of Marlowe and Wilder<sup>2</sup> yields a slope of  $-19.5 \text{ MPa/}^\circ\text{C}$ . Tropf and Harris<sup>1</sup> infer a pronounced softening of  $\text{Y}_2\text{O}_3$

at high temperature and a rapid non-linear decrease in elastic modulus at temperatures greater than 1200 °C. The present results do not support such a high order variation in elastic modulus, at least not within the temperature range of this study. The constants of Dickson and Anderson<sup>14</sup> and Marlowe and Wilder<sup>2</sup> are adiabatic while those of Price and Hubbert<sup>30</sup> are for constant temperature.

Elastic anisotropy for a cubic crystal may be characterized by the factor, A, computed using Eq. 5.

$$A = \frac{2C_{44} + C_{12}}{C_{11}} - 1 \quad (5)$$

The elastic constants measured here yield a value for A of  $0.170 \pm 0.015$ , while those of Aleksandrov et al. yield 0.212.<sup>15,16</sup> For comparison the values of A for MgO, BaO, and yttrium aluminum garnet ( $Y_3Al_5O_{12}$ , YAG) are 0.37, -0.07 and 0.02, respectively.<sup>16</sup>

The anisotropy does not vary significantly over the temperature range measured. There appears to be no systematic trend, and no variations in A within the error of the measurement. This contrasts with the behavior of several other oxides which show marked changes with temperature (Table V).

It is possible that this behavior simply results from a peculiarity of the interactions of Y and O, namely that they do not change substantially with temperature, but it is also possible that the constance of anisotropy with temperature is partially tied to the structure of yttria.

To a rough approximation, the elasticity of a crystal may be described by pair potentials between neighboring atoms and 3-body terms which give a potential energy based on the angle of two bonds attached to a central atom. For the halite structure, these may be related qualitatively to the macroscopic elasticity tensor. The halite structure consists of octahedra whose points are directed along the  $\langle 100 \rangle$  crystallographic directions.<sup>31</sup> Therefore, tension or compression along  $\langle 100 \rangle$  directions ( $C_{11}$ ) corresponds to a change in length of the bonds which are all directed toward the points of the octahedra (i.e.  $\langle 100 \rangle$  directions). Shear along the  $\langle 100 \rangle$  directions ( $C_{44}$ ), however, results in the bending of 3 atom groups. Therefore, to a first approximation, a change with temperature, of only the pair potentials between atoms would result in a change in  $C_{11}$  leaving  $C_{44}$  unaffected, and vice versa for a change in the 3-body term. Though oversimplified, this analysis suggests that the halite structure would show comparable changes in its macroscopic moduli and its fundamental atomic interactions (i.e. the relative resistance to bond stretching/compression as compared to 3-body bending).

Ytria also has 6-fold coordinated cations. Its structure (bixbyite), however, is much more complex than that of halite, with 16 formula units per cell, and the coordination polyhedra in yttria are not regular octahedra.<sup>31</sup> They are substantially deformed, and the structure is sometimes described as having cubic coordination for  $Y^{3+}$  with  $O^{2-}$  ions at opposite corners of the cube missing, essentially a defect fluorite structure.<sup>22,32</sup> Regardless of the description of the structure, the Y-O bonds point in many crystallographic directions. Therefore, unlike compounds with the halite structure, uniaxial forces along any crystallographic direction will involve both

stretching/compression of bonds and 3-body bending. Therefore, a change in relative resistance of one of these as compared to the other may produce a much smaller change in the macroscopic moduli and hence the anisotropy.

This hypothesis is supported by the relatively low change in anisotropy with temperature for other crystals with a complex relationship between bond directions and the unit cell. This is seen for YAG in Table V, and applies to several other garnets such as almandine and pyrope.<sup>16</sup> Like yttria, garnets have a complex crystal structure with irregular coordination polyhedra. Spinel also follows this trend with a relatively low value of  $dA/dT$ .<sup>16,33</sup> Various III-V compounds with zinc-blende lattices, such as GaAs or GaSb, and elements with diamond cubic lattices, such as diamond and silicon, show very low changes in anisotropy with temperature as well.<sup>16</sup> These structures also experience a combination of bond stretching/compression and 3-body bending, for both uniaxial tension and pure shear along high symmetry directions.

#### IV. Conclusions

The single-crystal elastic moduli of yttria were measured using Brillouin spectroscopy at room temperature and high temperatures ranging to 1200°C. The room temperature values differed significantly from previous single-crystal measurements,<sup>15,16</sup> but bulk properties calculated from the present study agree much more closely with most literature values reported for polycrystalline yttria.<sup>1,8,9,11,13</sup> This is important since it suggests that the elasticity of polycrystalline yttria ceramics can be accounted for by the elasticity of the  $Y_2O_3$  crystal lattice itself. No second phase or secondary effect is

indicated here as may have been suggested by the previous results. Sample misorientation in the previous study is offered as a potential reason for the discrepancy.

All elastic moduli display a modest linear decrease over the temperature range studied. The variation of bulk and shear moduli with temperature correspond closely to those reported for a  $91\text{Y}_2\text{O}_3 \cdot 9\text{ThO}_2$  compound.<sup>14</sup> Likewise, the change in Young's modulus with temperature agrees well with measurements on pure polycrystalline yttria.<sup>2</sup> Since accurate determinations of the temperature variation of properties for polycrystalline yttria ceramics have been made previously,<sup>2,14</sup> perhaps the more important addition of this study is the temperature dependence of elastic anisotropy, which was found to remain essentially constant for yttria as compared to significant changes for several other oxides with simpler cubic structures. A possible relation between the elastic anisotropy change with temperature and structure is proposed.

## Acknowledgements

The work of J. W. Palko was supported by the Fannie and John Hertz Foundation graduate fellowship. X-ray work was performed by J. McMillan at the Center for Microanalysis of Materials at UIUC. Thanks to D.C. Harris for help in obtaining certain reference matter. This work was partially supported by a United States Air Force Office of Scientific Research AASERT Grant, under contract number F49620-97-1-0427 and NSF grant EAR-96-14416.

## References

- 1 W. J. Tropf and D. C. Harris, Proc. SPIE **1112**, 9 (1989).
- 2 M. O. Marlowe and D. R. Wilder, J. Am. Ceram. Soc. **48**, 227 (1965).
- 3 R. L. Gentilman, Proc. SPIE **683**, 2 (1986).
- 4 W. H. Rhodes, G. C. Wei, and E. A. Trickett, Proc. SPIE **683**, 12 (1986).
- 5 A. Sayir, S. C. Farmer, P. O. Dikerson, and H. M. Yun, Mat. Res. Soc. Sym. Proc. **365**, 21 (1995).
- 6 E. K. Keler and A. B. Andreeva, Ogneupory, no.5, 224 (1963)[Refractories, no. 5, 243 (1963)].
- 7 W. R. Manning and J. Orville Hunter, J. Am. Ceram. Soc. **51**, 537 (1968).
- 8 W. R. Manning, J. O. Hunter, and J. B. R. Powell, J. Am. Ceram. Soc. **52**, 436 (1969).
- 9 K. K. Phani and S. K. Niyogi, J. Am. Ceram. Soc. **70**, C362 (1987).
- 10 G. C. Wei, C. Brecher, M. R. Pascucci, E. A. Trickett, and W. H. Rhodes, Proc. SPIE **929**, 50 (1988).
- 11 K. Shibata, H. Nakamura, and A. Fujii, Proc. SPIE **1326**, 48 (1990).
- 12 G. C. Wei, M. R. Pascucci, E. A. Trickett, S. Natansohn, and W. H. Rhodes, Proc. SPIE **1326**, 33 (1990).
- 13 O. Yeheskel and O. Tevet, J. Am. Ceram. Soc. **82**, 136 (1999).
- 14 R. W. Dickson and R. C. Anderson, J. Am. Ceram. Soc. **51**, 233 (1968).

- 15 V. I. Aleksandrov, V. F. Kitaeva, V. V. Osiko, N. N. Sobolev, V. M. Tatarintsev, and I. L. Chisty, *Sb. Kratk. Soobshch. Fiz. AN SSSR Fiz. Inst. P. N. Lebedeva*, no. 4, 8 (1976)[*Sov. Phys. Lebedev Inst. Rep.*, no. 4, 7 (1976)].
- 16 *Elastic, Piezoelectric, Pyroelectric, Piezooptic, Electrooptic Constants, and Nonlinear Dielectric Susceptibilities of Crystals; Vol. III/18*, edited by K.-H. Hellwege and O. Madelung (Springer-Verlag, Berlin, 1984).
- 17 G. B. Benedek and K. Fritsch, *Phys. Rev.* **149**, 647 (1966).
- 18 E. S. Zouboulis and M. Grimsditch, *J. Appl. Phys.* **70**, 772 (1991).
- 19 L. D. Landau and E. M. Lifshitz, *Theory of Elasticity* (Pergamon Press, London, 1959), p. 104.
- 20 J. F. Nye, *Physical Properties of Crystals: Their Representation by Tensors and Matrices* (Clarendon Press, Oxford, 1985), p. 114.
- 21 A. Sayir and S. C. Farmer, *Mat. Res. Soc. Sym. Proc.* **365**, 11 (1995).
- 22 D. Taylor, *Brit. Ceram. Trans. and J.* **83**, 92 (1984).
- 23 J. Palko, M.S. Thesis, University of Illinois, Urbana-Champaign, 2000.
- 24 J. D. Bass, *J. Geophys. Res.* **94**, 7621 (1989).
- 25 S. V. Sinogeikin, J. D. Bass, and T. Katsura, *J. Geophys. Res.* **103**, 20 (1998).
- 26 S. V. Sinogeikin, J. M. Jackson, B. O'Neill, J. W. Palko, and J. D. Bass, *Rev. Sci. Instrum.* **71**, 201 (2000).
- 27 D. J. Weidner and H. R. Carleton, *J. Geophys. Res.* **82**, 1334 (1977).

- 28 R. P. Ingel and D. Lewis, *J. Am. Ceram. Soc.* **71**, 261 (1988).
- 29 R. Vacher and L. Boyer, *Phys. Rev. B* **6**, 639 (1972).
- 30 M. W. Price and T. E. Hubbert, "Mechanical and Thermal Properties of Four IR Dome Materials," Southern Research Institute Report No. SRI-EAS-87-1272-6225, 1988 (unpublished see ref. 1).
- 31 R. W. G. Wyckoff, *Crystal Structures*, Vol. 2, 2 ed. (John Wiley & Sons, New York, 1963), p. 2.
- 32 M. G. Paton and E. N. Maslen, *Acta Crystallogr.* **19**, 307 (1965).
- 33 V. Askarpour, M. H. Manghnani, S. Fassbender, and A. Yoneda, *Phys. Chem. Miner.* **19**, 511 (1993).

Table I: Room temperature elastic constants of yttria

Modulus	This study	Aleksandrov, et al. <sup>15,16</sup>
$C_{11}$ (GPa)	$223.6 \pm 0.6$	227
$C_{44}$ (GPa)	$74.6 \pm 0.5$	68.6
$C_{12}$ (GPa)	$112.4 \pm 1.0$	138

Table II: Measured and calculated bulk properties of yttria at room conditions

K (GPa)	$G_V$ (GPa)	$G_R$ (GPa)	$G_{VRH}$ (GPa)	$G_{Polycrystal}$ (GPa)	Ref.
$149.5 \pm 1.0$	$67.0 \pm 0.8$	$65.6 \pm 0.8$	$66.3 \pm 0.8$		This Study
167.7	59.0	56.4	57.7		15,16
$148.9 \pm 3.0$				$69.2 \pm 2.0$	13
145				67	1
146.2				69.42	8

Table III: Measured elastic constants for yttria at elevated temperatures

T (°C)	C <sub>11</sub> (GPa)	C <sub>44</sub> (GPa)	C <sub>12</sub> (GPa)	K (GPa)	G <sub>VRH</sub> (GPa)
22 <sup>a</sup>	225.1	74.6	113.6	150.8	66.4
22 <sup>b</sup>	222.4	73.7	110.8	148.0	66.0
200	221.1	73.4	110.6	147.5	65.5
400	216.9	72.8	108.0	144.3	64.8
600	212.2	70.4	106.7	141.8	62.7
800 <sup>a</sup>	206.2	69.0	102.5	137.1	61.5
800 <sup>b</sup>	205.3	67.3	103.2	137.2	60.3
1000	199.1	65.3	99.5	132.7	58.6
1200	193.6	63.7	97.9	129.8	56.8

<sup>a</sup> Experimental run to 800°C. Errors for this run are  $\pm 0.7\%$  for C<sub>11</sub>,  $\pm 3.3\%$  for C<sub>44</sub>, and  $\pm 1.9\%$  for C<sub>12</sub>.

<sup>b</sup> Experimental run from 800°C to 1200°C. Errors for this run are  $\pm 0.9\%$  for C<sub>11</sub>,  $\pm 3.4\%$  for C<sub>44</sub>, and  $\pm 3.5\%$  for C<sub>12</sub>.

Table IV: Fitted temperature derivatives for single-crystal and bulk elastic properties of yttria

Modulus	Temperature Derivative (MPa/ °C)
$C_{11}$	$-26 \pm 3$
$C_{44}$	$-9 \pm 2$
$C_{12}$	$-13 \pm 2$
K	$-17 \pm 2$
$G_{\text{VRH}}$	$-8 \pm 2$

Table V: Comparison of changes in elasticity and anisotropy with temperature for several oxides

All temperature derivatives in ( $10^{-4}/K$ )	$Y_2O_3$ pres. study	MgO <sup>16</sup>	BaO <sup>16</sup>	$Y_3Al_5O_{12}$ (YAG) <sup>16</sup>
$(dC_{11}/dT)/C_{11}$	$-1.14 \pm 0.13$	-2.0	-3.7	-0.9
$(dC_{44}/dT)/C_{44}$	$-1.21 \pm 0.24$	-0.8	-1.16	-0.7
$(dC_{12}/dT)/C_{12}$	$-1.11 \pm 0.18$	0.7	0	-0.52
A	$0.170 \pm 0.015$	0.37	-0.07	0.02
dA/dT	$0 \pm 0.1$	2.1	2.8	0.3

Figure 1: Schematic of symmetric platelet scattering geometry

Figure 2: Room temperature velocities in the  $\{100\}$  plane of yttria.

Figure 3: Single-crystal elastic moduli at high temperature

Figure 4: Variation of the bulk modulus of yttria with temperature

Figure 5: Variation of the shear modulus of yttria with temperature

Figure 6: Variation of the Young's modulus of yttria with temperature.

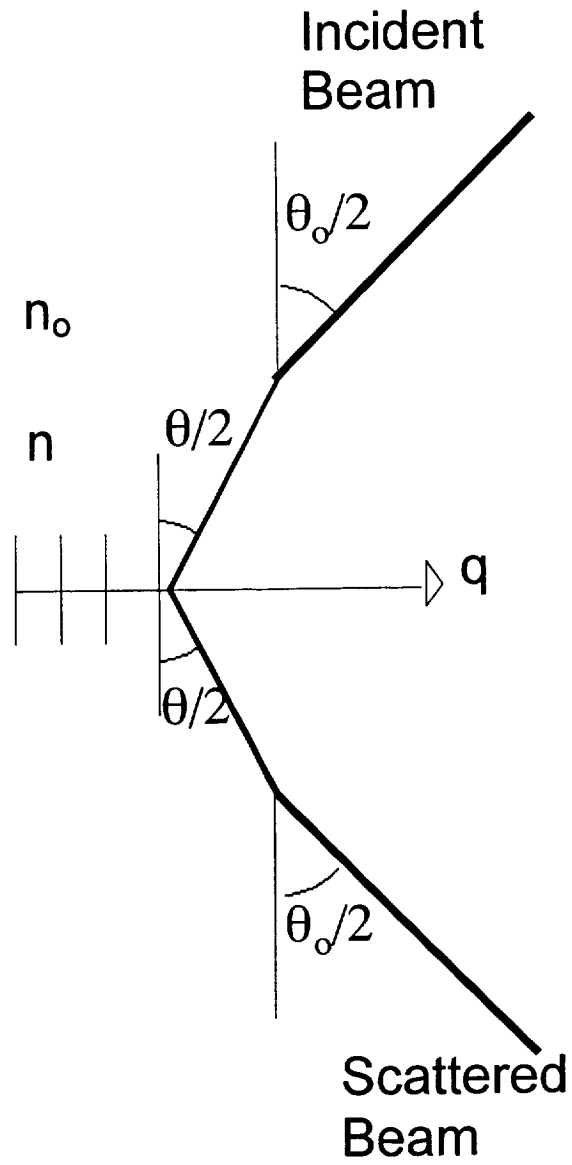


Figure 1 Palko, Kriven, Sinogeikin, Bass, Sayir (2000)

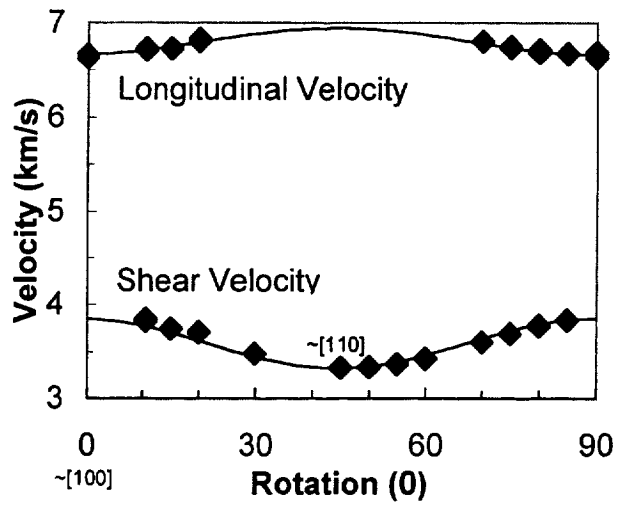


Figure 2 Palko, Kriven, Sinogeikin, Bass, Sayir (2000)

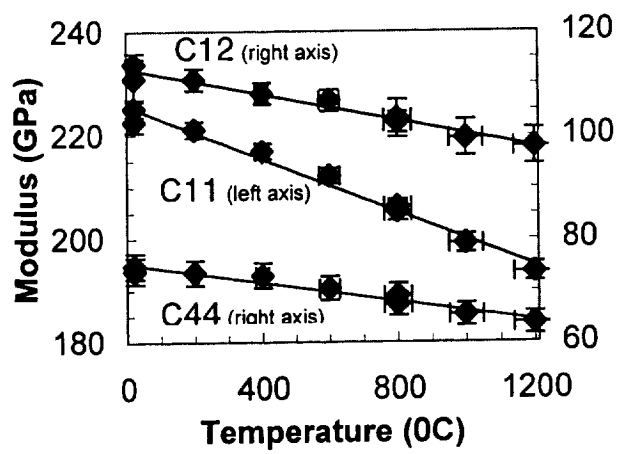


Figure 3 Palko, Kriven, Sinogeikin, Bass, Sayir (2000)

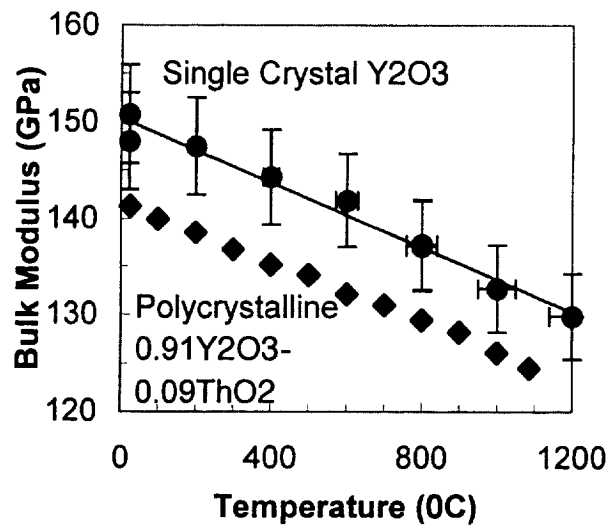


Figure 4 Palko, Kriven, Sinogeikin, Bass, Sayir (2000)

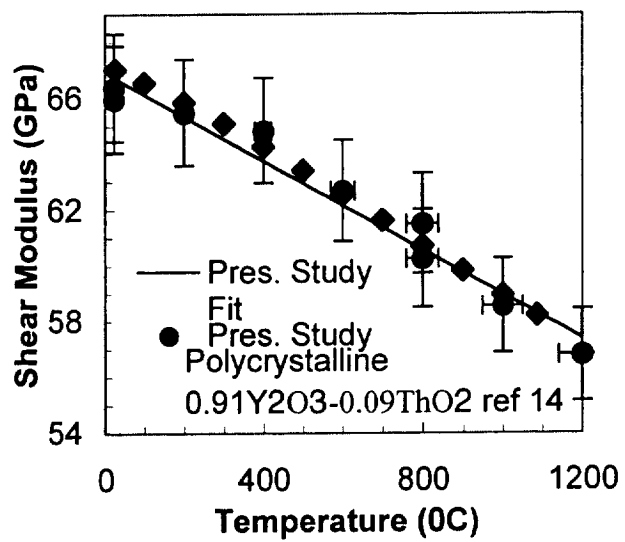


Figure 5 Palko, Kriven, Sinogeikin, Bass, Sayir (2000)

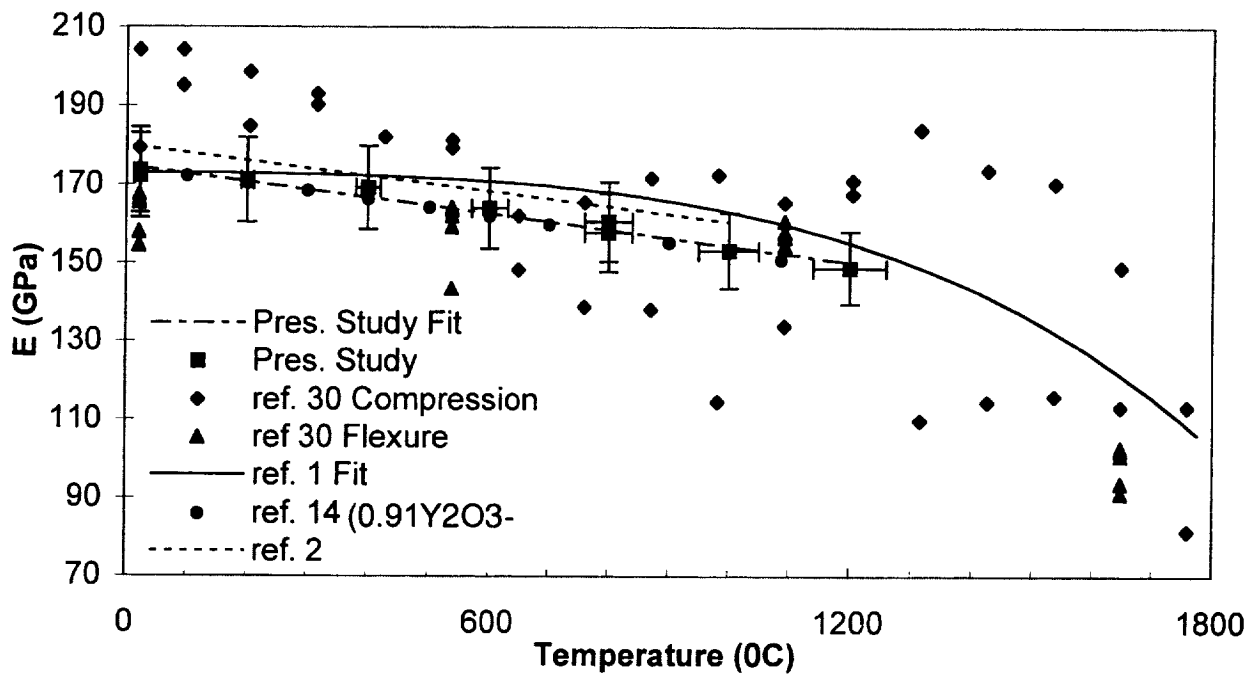


Figure 6 Palko, Kriven, Sinogeikin, Bass, Sayir (2000)